Analytical Investigation of Concrete Beam Reinforced with GFRP Rebars Under Low Axial Loading

Velkumar Senthil Kumar and Sadeghian Pedram

1 Introduction

Over the past few decades, concrete structures built with steel reinforcement in the humid and aggressive marine environment are more susceptible to corrosion. This results in steel reinforcement deterioration, reduced structural strength, maintenance cost increase, affects the performance and curtails the life span. After extensive research, Fiber-reinforced polymers (FRP) bars emerged as a suitable composite material to replace the steel reinforcement in the concrete structure and as a solution to overcome the severe problems due to corrosion. However, FRP bars have higher tensile strength compared to steel reinforcement, whereas the modulus of elasticity of FRP bars is much lower than its counterpart. The FRP bars in compression are relatively low compared to its tensile strength hence the contribution of FRP bars in compression should be completely ignored (ACI 440.1R-15). Based on CAN/CSA S806-12, GFRP bars can be used in the compression member if the contribution of GFRP bars in compressive strength is neglected.

It is believed that in the construction industry, the steel-reinforced concrete beams are being designed only for flexure, and any low accidental axial loads due to wind or seismic loads under 10% are being ignored. As the design codes and guidelines are more stringent on GFRP bars in compression, ignoring of low axial load in the beam subjected to flexure will cause the beam to design failure. Much research was conducted in the past to investigate GFRP beams, and this paper will focus on the analytical model to show the reduction in the ultimate bending capacity of the beam once low axial load in the range of 5–10% applied. For the FRP beams, most of the design codes recommend the over-reinforced section to get concrete crushing as the preferred mode of failure, which can yield a higher level of deformability [3].

V. S. Kumar (✉) · S. Pedram
Department of Civil and Resource Engineering, Dalhousie University, Dalhousie, Canada
e-mail: svelkumar@dal.ca

© Canadian Society for Civil Engineering 2023

S. Walbridge et al. (eds.), *Proceedings of the Canadian Society of Civil Engineering Annual Conference 2021*, Lecture Notes in Civil Engineering 241,
https://doi.org/10.1007/978-981-19-0511-7_38

Hence, the reinforcement ratio of 4% considered for the beam is over-reinforced, and concrete crushing is the expected mode of failure. This research's main objectives are to investigate the flexural behavior of concrete beams reinforced with GFRP bar subjected to low axial load by plotting the P-M interaction diagram based on the ultimate concrete strain of 3000 μmm/mm in the extreme concrete fiber.

2 Analytical Study

This section provides a brief outline of the model that was created to analyze the GFRP reinforced beam under bending and low axial compressive load. From the recent research, design codes, and guidelines, it is well known that the contribution of GFRP bars in compression was yet to be determined and hence the consideration in design is completely ignored. The outcome of the result presented from the analytical model demonstrates that ignoring the low axial compressive load in the GFRP reinforced beam subjected to flexure causes design failure. The effect of axial compressive load should be considered while finding the bending capacity of the GFRP beam, which directly affects the strength of the real beam.

2.1 Model Description

In accordance with ACI 440.1R-15 and CSA S806-12 design provisions and guidelines, a model was developed to determine the moment capacity of the beam under low axial load to plot the axial load versus bending moment interaction diagram. In the computation of axial load and bending moment, the same procedure as a concrete beam with steel reinforcement was followed for the GFRP beam. However, the interaction diagram will not be similar to the steel-reinforced beam due to non-linear material behavior.

Figure 1 explains the concrete model proposed in this paper with strain profile and parabolic stress diagram using appropriate symbols. The cross-section of the

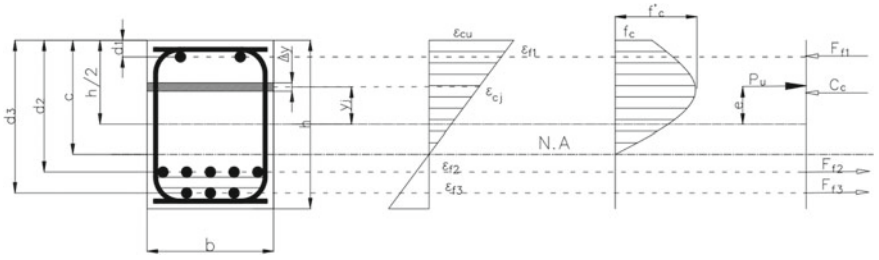

Fig. 1 Stress and strain profile of GFRP beam cross-section

beam consists of three layers of longitudinal reinforcement out of which one layer is top compression reinforcement, and two layers are bottom tension reinforcement. In the below figure, beam length, width, cross-sectional area, effective depth, location of the rebar layer, and neutral axis are represented in a short form as "b", "h", "A", "d", "d1" and "c". where ε_{cu} is the ultimate concrete strain, ε_{cj} is the axial strain of concrete fiber, ε_{fi} is the axial strain of GFRP, f'_c is the unconfined concrete maximum compressive stress, and f_{ci} is the concrete stress corresponding to the axial strain of concrete fiber.

2.2 Assumptions

In CSA S806-12, it was mentioned that FRP bars can be used as compression member without considering the compressive strength of the bar in design whereas ACI 440.1R-15 completely avoid relying upon FRP bars to resist the compressive forces because of lower elastic modulus. The beginning step of the analytical model will be a cross-sectional analysis of GFRP beam subjected to combined flexure and axial compression experience the strain gradient that was determined using the stress–strain curve method by dividing the cross-section of the beam into 20 segments of concrete fiber with equal thickness. In this model, concrete is considered only to resist the compression while the tensile stress in concrete is completely ignored and hence the concrete below the neutral axis is assumed to be cracked with no contribution to moment resistance. Full composite action exists between concrete and GFRP, which makes the strain profile linear from the top end of the beam's compressive face to the bottom tensile face of the beam. The extreme concrete fiber ultimate strain is considered as 3000 μmm/mm as per ACI 440.1R-15, and the maximum strain limit of GFRP bars was calculated as 13,000 μmm/mm based on ultimate tensile strength and modulus of elasticity of GFRB bars.

2.3 Analytical Procedure

In this section, first step will be to determine the ultimate axial strain of the GFRP bars and the axial strain of the GFRP bars in each reinforcement layer will be computed to determine the axial compressive force (P_u) and its corresponding bending moment. The ultimate axial strain (ε_{fi}) is determined for every neutral axis depth out of 20 neutral axis depth assumed for the beam section using the following equation:

$$\varepsilon_{fi} = \frac{\varepsilon_{cj}}{\varepsilon_{cu}}\left(c_q - d_i\right) \tag{1}$$

where c_q is the neutral axis of the beam section and d_i is the depth of each reinforcement layer. The stress–strain method was used in the cross-sectional analysis of the

GFRP beam. In 1973, Popovics proposed the expression to determine the concrete in compression which predicted the ascending part of the stress–strain curve accurately was slightly modified and proposed by [6] including the k factor to exactly predict the descending part of the stress–strain curve, as shown in the following equation:

$$f_{cj} = f'_c \frac{\varepsilon_{cj}}{\varepsilon'_c} \frac{n}{n - 1 + (\varepsilon_{cj}/\varepsilon'_c)^{nk}} \tag{2}$$

where n is the curve fitting factor governing for ascending slope, k is the curve fitting factor governing for descending slope, and ε'_c is the concrete strain when f_c reaches the maximum compressive stress f'_c are calculated as:

$$n = 0.8 + \frac{f'_c}{17}(\text{MPa}) \tag{3}$$

$$k = 0.67 + \frac{f'_c}{62}(\text{MPa}) \tag{4}$$

$$\varepsilon'_c = \frac{f'_c}{E_c} \frac{n}{n - 1} \tag{5}$$

The axial compression or tension force in the GFRP bar is linear with the same modulus of elasticity and will be determined by multiplying the are of GFRP bars using the following equation:

$$F_{fi} = E_f \varepsilon_{fi} A_{fi} \tag{6}$$

where F_{fi} and A_{fi} are the axial force and gross area of GFRP bars, respectively. The total axial compressive force of the beam section will be the summation of compressive force due to the concrete fibers and the axial force due to the GFRP bars in the compression zone of the beam section. The bending moment due to the axial compressive force in each concrete fiber above the neutral axis will be determined by multiplying the beam width, segment thickness (Δy), and the lever arm from the center of the section (h/2). The total bending moment will be the summation of the bending moment due to the forces in concrete fibers and the moment due to the axial force in GFRP bars located within the compression zone of the beam section. The ultimate axial (P_u) and bending moment (M_u) are determined as shown in the following:

$$P_u = \sum_{j=1}^{20} f_{cj} b \Delta y - \sum_{i=1}^{3} F_{fi} \tag{7}$$

$$M_u = \sum_{j=1}^{20} f_{cj} b \Delta y (h/2 - c) - \sum_{i=1}^{3} F_{fi} (h/2 - d_i) \tag{8}$$

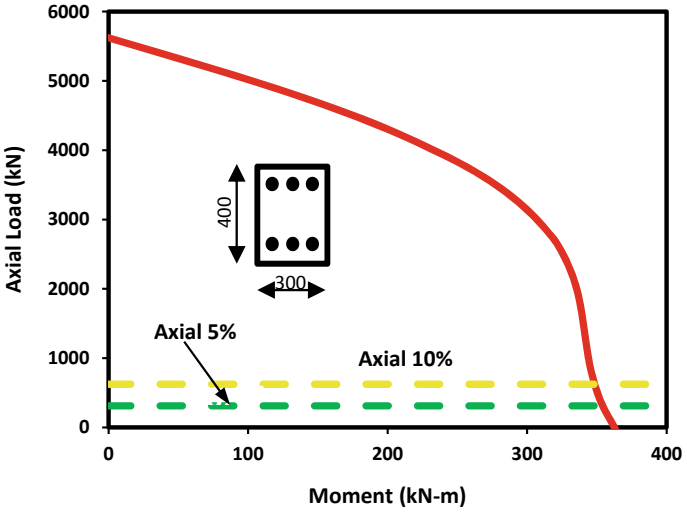

Fig. 2 Analytical model—beam interaction diagram (Axial load vs bending moment)

The above-mentioned procedure is repeated for the different values of the neutral axis to determine the axial and the corresponding moment of the beam Sect. 300 mm × 400 mm to form the P-M interaction diagram. The material properties used were #8 (25 mm) diameter longitudinal GFRP bars of 506.7 mm2 nominal area and #3 (10 mm) diameter GFRP bars were considered as shear reinforcement. The concrete compressive strength of 40 MPa with 25 mm cover, ultimate tensile strength, and elastic modulus of GFRP bars was considered as 620 MPa and 46 GPa, respectively. Based on the beam section and material properties, P-M interaction diagram was plotted as shown in Fig. 2, comparing with the low axial load of 5.0 and 10.0% plotted as a horizontal line indicating the reduction of bending resistance at this particular axial load levels.

2.4 Verification

In this first verification section, the analytical model developed was verified against the experimental test data and analytical model of the research performed by [4] where they have investigated ten concrete rectangular columns with the cross-sectional size of 205 mm × 306 mm having longitudinal reinforcement of #6 GFRP bars, reinforcement ratio of 2.78 and 4.80% were casted with concrete compressive strength of 48.4 MPa. The analytical model developed by [4] was based on Popovics stress–strain curve method, which in comparison with the analytical model developed using [6] in Fig. 3. shows that the predicted P-M interaction diagram is in reasonable agreement with the experimental test data.

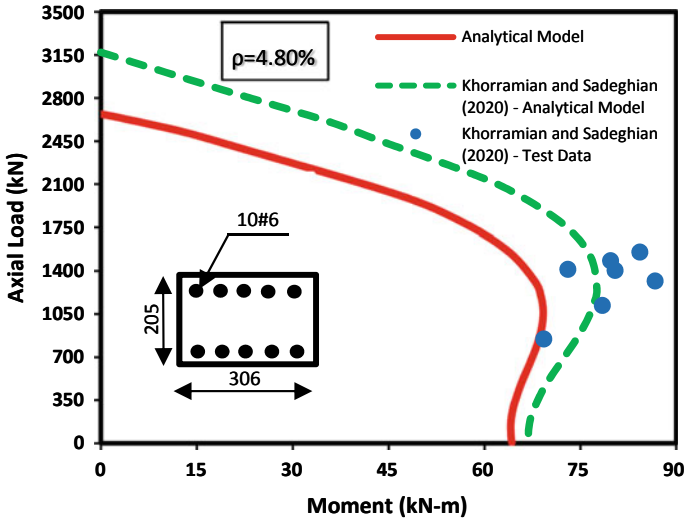

Fig. 3 Beam interaction diagram—axial load vs bending moment [4]

In this second verification section, the analytical model developed was verified against the experimental test data and analytical model of the research performed by [5] to study the axial-flexural performance of high strength concrete bridge compression members reinforced with Basal reinforced polymer (BFRP) bars. Eight square columns of cross-sectional size 400 mm × 400 mm × 2000 mm were casted, and an analytical study was performed with varying concrete strength, reinforcement ratio, and load eccentricity. The model was precisely developed using the stress–strain curve method proposed by [6]. The cross-sectional analysis was based on the design provision of ACI 440.1R-15 and CSA S806-12, considering the maximum concrete strain of 3500 μmm/mm as per CSA S806-12. The main objective of this research was to predict the axial and flexural strength, which was compared by plotting the axial moment interaction diagram and load-eccentricity, which was verified against the experimental investigation.

The analytical model was verified against [5] with the same beam cross-section, concrete strength 71.2 MPa, BFRP tensile strength 1646 MPa, elastic modulus 63.7 GPa, and all other parameters were used the same as specified. The input data was applied in the developed model, and the P-M interaction diagram comparison was plotted as shown in Fig. 4. as against [5] experimental data and analytical model. The curve fitting factor proposed by [6] was most accurate in predicting the descending branch of the stress–strain curve, which created the correction in the trend of the P-M interaction diagram specifically at the lower portion of the curve, which is tension controlled by BFRP bars whereas the impact in the upper portion of the curve controlled by concrete compression is negligible. The axial load and bending moment curve shown that the result predicted from the analytical model is in good agreement with [5].

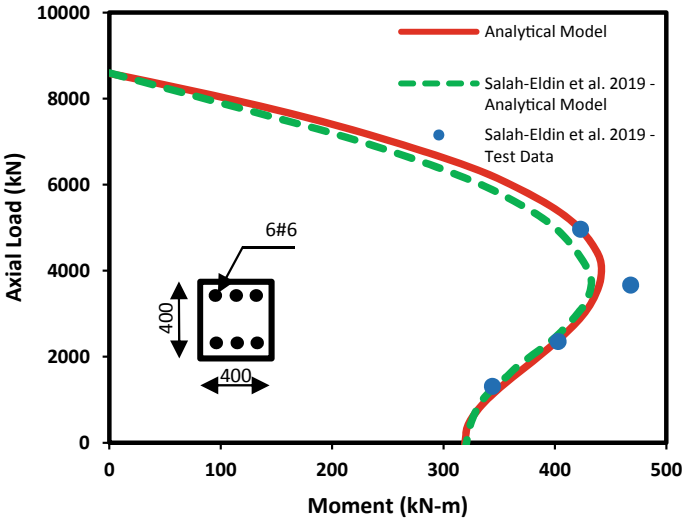

Fig. 4 Beam interaction diagram—axial load vs bending moment [5]

3 Parmetric Study

The analytical model was used to conduct the parametric study to assess the effect of three significant parameters using cross-sectional analysis in the behavior of the GFRP reinforced beam. The parameters used in the investigations were reinforcement ratio, concrete strengths, and axial load. The beam cross-section considered were 300 mm × 400 mm with varying reinforcement ratios of 3, 4, and 5%, concrete strength of 40–60 MPa, and the axial load at 5.0 and 10.0% capacity of the beam were compared and studied. The material properties used were #8 (25 mm) diameter longitudinal GFRP bars of 506.7 mm^2 nominal area and #3 (10 mm) diameter GFRP bars were considered as shear reinforcement. The ultimate tensile strength and elastic modulus of GFRP bars were considered as 620 MPa and 46 GPa, respectively. The increase of reinforcement ratio from 3 to 5% in the bottom side of the beam with the concrete strength of 60 MPa shows that bending moment resistance of beam increases from 323 to 450 kNm in the tension-controlled section. The compression reinforcement that was considered is similar in all cases shows that the curve remains identical at the top portion of the beam, which is a compression-controlled zone, and the curve changes consistently at the bottom portion of the beam. Moreover, at the lower reinforcement ratio, the lower end of the curve shows a steep decline rather than the gradual decline of the curve at a higher reinforcement ratio (Fig. 5).

The variation in concrete strength have resulted in the large interaction curve of not just increasing the bending resistance but changes the axial capacity of uncracked concrete. The axial load–bending moment interaction curves for each concrete strength (f'_c) have enlarged in size gradually without affecting the trend of the curve. The effect of reinforcement ratio gives a clear indication that the failure of

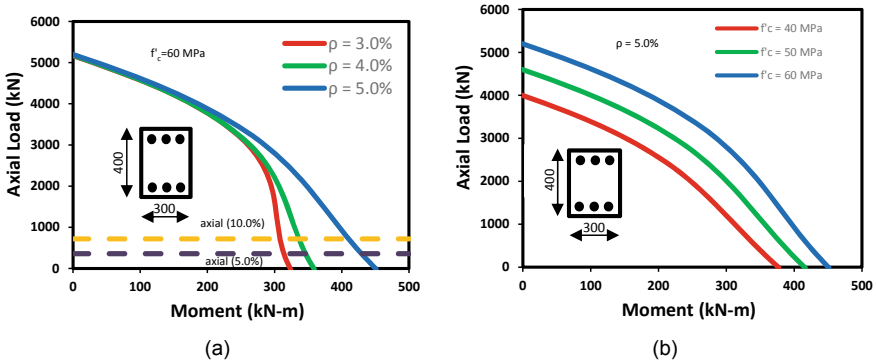

Fig. 5 Beam interaction diagram—**a** effect of reinforcement ratio **b** effect of concrete strength

the beam can occur because of applying a minimum accidental axial load of 5.0% and the effect is more pronounced at a higher reinforcement ratio while it is minimum at a lower reinforcement ratio. Thus, parametric investigation paved the way to arrive at a number of predominant conclusions in the behavior of concrete beam reinforced with GFRP bars, and one of the key findings is the effect of concrete strength parameter plays an insignificant role in comparison with the effect of reinforcement ratio which causes the direct impact in reducing the beam strength due to any axial load.

4 Conclusion

This study was performed to investigate the flexural behavior of glass fiber reinforced polymer (GFRP) bars in the concrete beam with the analytical model developed with Mathcad Prime 2.0. The model considered the contribution of FRP bars in compression up to the ultimate concrete strain of extreme concrete fiber as 3000 μmm/mm. The verification of the model against [4] and [5] were in reasonable agreement, which confirmed the accuracy of the analytical model. From the P-M interaction diagram of the analytical model and parametric study, it was evident that the ultimate bending resistance of the beam decreased from 363 kN-m to 354 kN-m at a lower axial load of 5%, whereas the decrease was 363–348 kN-m at an axial load of 10%, hence the low axial load in designing the GFRP beam for flexure should no longer be ignored. However, as this is ongoing research, an experimental study will be conducted to verify the analytical model further.

References

1. ACI 440.1R (2015) Guide for the design and construction of structural concrete reinforced with fiber-reinforced polymers (FRP) bars. American Concrete Institute, Farmington Hills, MI, USA
2. CAN/CSA S806–12 (2012) Code for the design and construction of building structures with fiber-reinforced polymers. Canadian Standards Association, Mississauga, ON, Canada
3. El-Nemr A, Ahmed EA, Benmokrane B (2019) Flexural behavior and serviceability of normal and high-strength concrete beams reinforced with glass fiber-reinforced polymer bars. ACI Struct J 110-S88
4. Khorramian K, Sadeghian P (2020) Experimental investigation of short and slender rectangular concrete columns reinforced with GFRP bars under eccentric axial loads. J Compos Constr 24(6):04020072
5. Salah-Eldin A, Mohamed HM, Benmokrane B (2019) Axial-flexural performance of high-strength-concrete bridge compression members reinforced with basalt-FRP bars and ties: experimental and theoretical investigation. J Bridg Eng 24(7):04019069
6. Thorenfeldt E, Tomaszewicz A, Jensen JJ (1987) Mechanical properties of high strength concrete and application to design. Symposium proceedings utilization of high-strength concrete. Trondheim, Norway, pp 149–159